Interdisciplinary Studies on Applied Science, 3(1):20–29, 2026. DOI: 10.58613/isas312

Interdisciplinary Studies on Applied Science

Journal homepage: https://www.gpub.org/journal-details.php?journal-id=42

ISSN (E): 3048-877X

Research Article

Design, Synthesis, and Biological Activity of Novel 1,2,3-Triazole Hybrids as Potent Antimicrobial

Alaa K. Shanshal [1], Faten Jassim Mohammed [2], Ahmed Ridha Abduljawad[3], Akhlas yousif hasan[2] and Ali Jabbar Radhi [4,5*]

[1]*General Directorate of Education, Third Rusafa, Baghdad, Ministry of Education, Baghdad, Iraq.*
[2]*Department of Pharmacognosy, Faculty of Pharmacy, University of Kufa, Najaf, Iraq.*
[3]*Faculty of Medical Technologies, Islamic University, Najaf, Iraq.*
[4]*College of Pharmacy, University of Alkafeel, Najaf, Iraq.*
[5]*ARCPMS University of AlKafeel, Najaf, Iraq.*
[*]*Corresponding author: alijebar56@alkafeel.edu.iq*

Article Info

Keywords: *Click chemistry, Antimicrobial activity, Molecular docking, ADMET analysis, Drug-likeness, Antimicrobial resistance (AMR).*

Received: *18.12.2025;*
Accepted: *20.01.2026;*
Published: *01.02.2026*

Abstract

Antimicrobial resistance (AMR) and biofilm-associated infections remain core drivers of the global health crisis. New antimicrobial scaffolds that can deliver enhanced efficacy with low toxicity are needed [1]. A series of rationally designed indole 1,2,3-triazole hybrid derivatives (3ta-3te) were synthesized via efficient N-propargylation followed by Cu(I)-catalyzed azide-alkyne cycloaddition or click reaction. The structure was elucidated by IR, 1H & 13C NMR plus melting point analysis which confirmed successful formation of the targeted hybrids. Antibacterial/antibiofilm activities against S.aureus & B.subtilis/E.coli revealed that sulfonamide containing derivatives; 3td & most potently active te exhibited MIC values as low as 6.21μ M coupled with strong bactericidal effects! Molecular docking on S.aureus 4DUH showed high binding affinity scores (-8.07 to -8.39 kcal mol^{-1}) for both compounds where they formed important H-bond/ π-cation interactions (ARG136 catalytic residue) & ASP73 with biological results ADMET profiling highlighted positive physicochemical, pharmacokinetic and drug-likeness properties associated with oral administration among which 3te can be considered as a potential lead candidate. The results of the present study revealed that hybridization of triazole and indole pharmacophores resulted in enhanced antibacterial and antibiofilm activity, hence establishing them as scaffold platforms for next-generation antimicrobial agents.

1. Introduction

The scientists were happy to think that the innovation of antimicrobial drugs would terminate microbial infections. Later, resistance disappointed them in this belief [1]. Antimicrobial resistance is triggered by biofilm formation and misuse or overuse of easily available antimicrobial drugs [2]. Biofilms can be defined as an accumulation of microbial cells surrounded by a material of polymeric compounds produced by these microorganisms themselves [3]. Antibiotic biofilms are very hard and challenging to eradicate because they are resistant to antibiotics [4]. More than 75% of human microbial infections can be attributed to rapidly growing and colonizing pathogens inside human bodies that multiply antimicrobial resistant biofilm's pathogens [5, 6]. WHO reports confirmed that 1.27 million people died due to antimicrobial resistance in 2019, while this resistance caused approximately 4.95 million deaths worldwide [7]. Research on developing new antibiotics had sharply declined in the last few decades. This added negative consequence to AMR [8, 9]. Improper and extended

How To Cite: A.K. Shanshal, F.J. Mohammed, A.R. Abduljawad, A.Y. Hasan, A.J. Radhi. Design, Synthesis, and Biological Activity of Novel 1,2,3-Triazole Hybrids as Potent Antimicrobial. *Interdisciplinary Studies on Applied Science*, 3(1):20–29, 2026. https://doi.org/10.58613/isas312

use of antimicrobials has given a boost to AMR, therefore increasing health-care costs [10, 11]. Plans should immediately be made and implemented to fight AMR [12]. Molecular hybridization is defined as the rational design of pharmacophores with new multiple functions by covalently binding within the same structural framework, two or more pharmacophoric subunits that belong to different bioactive molecules [13]. A hybrid molecule may have resultant cooperative binding and efficacy better than its parents besides exhibiting lower side effects because it selectively binds specific targets (receptors). Other advantages found in literature reports. Indole also known as benzopyrrole is an important aromatic heterocyclic scaffold both found naturally occurring biologically active compounds synthetic ones too. Indoles have emerged as highly important antimicrobial agents in the field of medicinal chemistry because their derivatives display a wide range antibacterial activities against various strains tested [14, 15]. Over the past two decades 1,2,3-triazoles attracted much interest among medicinal chemists due to their broad-spectrum activity and easier synthetic accessibility via Cu(I)-catalyzed alkyne-azide cycloaddition reactions. Click chemistry has recently been applied as a biorthogonal reaction within biological and medicinal research fields [16, 17]. High yielding powerful selective reactions with extreme stereospecificity which assemble small units through heteroatom links resulting in 1,4-disubstituted 1,2,3-triazoles for various applications have been developed [18–22]. Pharmaceuticals specifically, display apparently enormous ranges of biological properties from antimicrobial [23–26], anticancer [27], antiviral [28], anti-inflammatory [29], antimalarial [30], anti-HIV [31], antidiabetic [32], antioxidant [33]. The present work is focused on the design conceptually novel indole-1,2,3-triazole hybrids to overcome antimicrobial resistance and biofilm-associated infections. By click chemistry combination of indole and triazole scaffolds the enhancement of antibacterial activity together with strong protein binding and good drug-like properties was aimed. Both biological testing and computational analysis underlined the sulfonamide-linked derivatives especially compound 3te as promising leads for developing next-generation antimicrobial agents.

2. Experimental Part

Unless otherwise stated, all reagents and solvents used in this work were obtained from commercial suppliers and used without further purification. The progress of the reaction was monitored by TLC using silica plates under UV light [34]. Elution was carried out on a column of silica gel (60-120 mesh) [35]. The melting points have been determined in open capillaries and are uncorrected. IR spectra were recorded with KBr pellets on Perkin Elmer RXI FT-IR system. 1H and 13C NMR spectra were run in DMSO – d_6 at 400 MHz and 100 MHz, respectively, using TMS as an internal standard; chemical shifts (δ) are reported downfield from TMS.

2.1. Synthesis of Compound (2)

A mixture containing compound (1) (1 mmol) and dry acetone (10 mL) was placed in a flask to which finely powdered potassium carbonate (2.5 mmol) was added, then addition of propargyl bromide (1.2-1.5 mmol) dropwise with stirring. The reaction mixture was refluxed for 3-6 hours until completion monitored by TLC. Allowed to cool to room temperature and filtered off inorganic salts, the filtrate was concentrated under reduced pressure. The residue extracted with ethyl acetate, washed water then brines dried by using anhydrous sodium sulfate filtered evaporated crude product purified by utilize column chromatography using suitable hexane/ethyl acetate gradient elution affords the N-propargylated product (2).

1-((prop-2-yn-1-yloxy)methyl)-1H-benzo[d][1,2,3]triazole (2):

Yield: 83% ; pale-whit solid, mp 127-129°C; IR (cm^{-1}), 3311 ($\equiv C-H$ stretch of terminal alkyne ($C \equiv C$–H), 3088 (C–H stretching aromatic rings), 2128 ($-C \equiv C$ stretch, alkyne), 1593 (aromatic C=C); ^1H NMR (400 MHz, DMSO – d_6) δ 7.69-7.34(m, 6H, Ar-H), 5.46(s, 2H, CH_2 attached to indole), 4.17 (s, 2H, CH_2 linked to alkyne); 13C NMR (100 MHz, DMSO – d_6) δ 136.69, 130.70, 128.27, 124.83, 122.92, 121.05, 112.92, 105.28, (6C, of aromatic carbons), 81.36 ($1C, C \equiv$), 76.27(1C, CH_2 linked to indole), 74.14 ($1C, \equiv C$–H), 56.76 (1C, CH_2 attached to terminal alkyne).

2.2. General procedure for the synthesis of 1,2,3-triazole derivatives (3ta-3te)

In a 25 mL round-bottom flask equipped with a magnetic stir bar, place the N-propargyl indole (2) (1.00 mmol) and the organic azide (1.10 mmol) and add a mixture of ethanol/water (4:1, total ca. 5–10 mL) to dissolve the reagents; then add copper (II) sulfate pentahydrate ($CuSO_4 \cdot 5H_2O$, 0.10 mmol) and sodium ascorbate (0.20 mmol) to generate the active Cu(I) catalyst in situ. Heat the reaction mixture to 70–75 °C with stirring and monitor progress by TLC, typical reaction time is 4 h until complete consumption of the alkyne. After completion, cool to room temperature, add ethyl acetate (20–30 mL), and filter the mixture through a pad of Celite to remove copper salts. Separate the organic phase, wash with water (2 × 15 mL) and brine (15 mL), dry over anhydrous Na_2So_4, filter and concentrate under reduced pressure. Purify the crude residue by flash column chromatography on silica gel (hexane/EtOAc) to afford the 1,4-disubstituted 1,2,3-triazole product (3ta–3te). Handle azides with caution (work on small scale, avoid concentrated inorganic azides and strong heating), and dispose of copper-containing waste according to institutional regulations.

1-(((1-(4-methoxyphenyl)-1H-1,2,3-triazol-4-yl)methoxy)methyl)-1H-indole (3ta):

75% ; yellow solid, mp 214-216 °C; IR (cm^{-1}), 3112(C-H of triazole ring), 3054 (aromatic C–H stretching, aromatic rings), 1577 (aromatic C=C); ^{1}H NMR (400 MHz, DMSO – d_6) δ 8.38 (s, 1H, 1,2,3-triazole-H), 7.64-7.01 (m, 10H, Ar-H),5.63 (s, 2H, CH_2 attached to indole), 4.61 (s, 2H, CH_2 linked to 1,2,3-triazole), 3.85(s, 3H, CH_3 methoxy) ; 13C NMR (100 MHz, DMSO – d_6) δ 149.24,120.54 (2C, C4 and C5 of triazole ring), 157.76, 136.53, 129.78, 128.89, 128.44, 123.39, 121.70, 120.99, 118.94, 115.99, 110.93, 103.26, (14C, of aromatic carbons), 73.97 (1C, CH_2 attached to indole), 59.12 (1C, CH_2 linked to 1,2,3-triazole), 55.24 (1C, CH_3 methoxy).

N-(4-(4-(((1H-indol-1-yl)methoxy)methyl)-1H-1,2,3-triazol-1-yl)phenyl)acetamide (3tb):

81% ; pale-brown solid, mp 187-189 °C; IR (cm^{-1}), 3322 (NH acetamide), 3125(C-H of 1,2,3-triazole ring), 3074 (aromatic C–H stretching, aromatic rings), 1687 (carbonyl of acetamide group), 1579(aromatic C=C); ^{1}H NMR (400 MHz, DMSO – d_6) δ 9.97(s, 1H, NH acetamide), (8.22 (s, 1H, 1,2,3-triazole-H), 7.61-6.79 (m, 10H, Ar-H),5.69 (s, 2H, CH_2 attached to indole), 4.69 (s, 2H, CH_2 linked to 1,2,3-triazole), 2.13 (s, 3H, CH_3 acetamide); 13C NMR (100 MHz, DMSO – d_6) δ 168.35 (1C, carbonyl of acetamide), 148.14, 120.65 (2C, C4 and C5 of 1,2,3-triazole ring), 136.41, 133.97, 131.28, 128.91, 128.45, 123.47, 122.21, 121.04, 120.02, 117.77, 111.89, 104.35, (14C, of aromatic carbons), 75.54 (1C, CH_2 attached to indole), 57.24 (1C, CH_2 linked to 1,2,3-triazole), 24.21(1C, CH_3 acetamide).

4-(4-(((1H-indol-1-yl)methoxy)methyl)-1H-1,2,3-triazol-1-yl)phenol (3tc):

75% ; pale-whit solid, mp 261-263 °C; IR (cm^{-1}), 3369 (O–H stretch of phenol), 3137 (C-H of 1,2,3-triazole ring), 3087 (aromatic C–H stretching, aromatic rings), 1592(aromatic C=C); ^{1}H NMR (400 MHz, DMSO – d_6) δ 9.54 (s, 1H, phenol-H), 8.19 (s, 1H, 1,2,3-triazole-H), 7.59-6.84 (m, 10H, Ar-H), 5.67 (s, 2H, CH_2 attached to indole), 4.59 (s, 2H, CH_2 linked to 1,2,3-triazole); 13C NMR (100 MHz, DMSO – d_6) δ 147.97,119.78 (2C, C4 and C5 of 1,2,3-triazole ring), 156.78, 136.98, 130.14, 129.14, 127.34, 123.87, 121.33, 120.24, 118.67, 115.94, 112.24, 103.86, (14C, of aromatic carbons), 75.13 (1C, CH_2 attached to indole), 57.65 (1C, CH_2 linked to 1,2,3-triazole).

4-(4-(((1H-indol-1-yl)methoxy)methyl)-1H-1,2,3-triazol-1-yl)-N-(pyrimidin-2-yl)benzenesulfonamide (3td):

73% ; Off-yellow solid, mp 232-234 °C; IR (cm^{-1}), 3287 (N–H stretch of sulfonamide), 3143(C-H of 1,2,3-triazole ring), 3065 (aromatic C–H stretching, aromatic rings), 1579 (aromatic C=C); ^{1}H NMR (400 MHz, DMSO – d_6) δ 11.21 (s, 1H, N-H sulfonamide), 8.25 (s, 1H, 1,2,3-triazole-H), 7.73-6.93 (m, 13H, Ar-H), 5.67 (s, 2H, CH_2 attached to indole), 4.58 (s, 2H, CH_2 linked to 1,2,3-triazole); 13C NMR (100 MHz, DMSO – d_6) δ 147.24, 120.57 (2C, C4 and C5 of 1,2,3-triazole ring), 157.14, 156.04, 139.87, 137.35, 136.14, 131.51, 129.92, 127.47, 123.26, 122.91, 121.98, 117.67, 112.57, 110.45, 104.56, (18C, of aromatic carbons), 75.14 (1C, CH_2 attached to indole), 59.11 (1C, CH_2 linked to 1,2,3-triazole).

4-(4-(((1H-indol-1-yl)methoxy)methyl)-1H-1,2,3-triazol-1-yl)-N-(5-methylisoxazol-3-yl)benzenesulfonamide (3te):

77% ; pale-white solid, mp 211-213 °C; IR (cm^{-1}), 3287 (N–H stretch of sulfonamide), 3124(C-H of 1,2,3-triazole ring), 3095 (aromatic C–H stretching, aromatic rings), 1588 (aromatic C=C); ^{1}H NMR (400 MHz, DMSO – d_6) δ 11.29 (s, 1H, N-H sulfonamide), 8.27 (s, 1H, 1,2,3-triazole-H), 7.83-7.03 (m, 10H, Ar-H), 6.14(s, 1H, CH, isoxazole), 5.62 (s, 2H, CH_2 attached to indole), 4.66 (s, 2H, CH_2 linked to 1,2,3-triazole), 2.35(s, 3H, CH_3 attached to isoxazole), ; 13C NMR (100 MHz, DMSO – d_6) δ 167.89, 156.47, 96.64 (3C, C5, C3 and C4 of isoxazole ring), 144.54,120.57 (2C, C4 and C5 of 1,2,3-triazole ring), 139.68, 137.70, 136.51, 131.63, 129.92, 127.47, 123.26, 121.91, 118.55, 116.67, 111.02, 103.56, (14C, of aromatic carbons), 75.08 (1C, CH_2 attached to triazole), 58.89 (1C, CH_2 linked to benzotriazole), 12.97 (1C, CH_3 linked to isoxazole).

2.3. Biological assays

Pathogenic strains used to test the antimicrobial activity of synthesized compounds (3ta-3te) were grown overnight, antibacterial strains in Mueller-Hinton Broth (MHB) at 37 °C and antifungal strains in potato dextrose broth at 28°C. All microbial suspensions were adjusted finally to a concentration of 1.5×10^6 CFU/mL for primary screening of the compounds at a concentration of 128 μ M. Test compounds were dissolved in DMSO and dispensed into 96 well microtiter plates (Genetix Biotech Asia Pvt. Ltd., India). The compound or compounds which showed inhibitory activity against any tested pathogen was further tested by two-fold serial dilution method according to CLSI guidelines [18] in secondary screening where serial dilutions gave final concentrations as follows:128,64,32,16 ,8 ,4 ,2 and 1 μ M. Wells containing only microbial inoculum served as negative controls. The MICs were read visually after incubation at 37 °C for 24 h (bacterial strains) and at 28 °C (fungal strains). Ciprofloxacin was used as a positive control in the antibacterial assay and nystatin in the antifungal assay.

The assay was run on biofilm-forming strains to test the activity of synthesized derivatives against antibiofilm. The test compound was incubated with bacterial cultures (initial inoculum of 10^5 CFU/mL) in 96-well polystyrene plates containing tryptic soy broth, 1% glucose added, making a final volume per well of 200 μ L. The plates were then incubated at 37 °C while Candida albicans plates were incubated at 28 °C for 48 h under static conditions. The assay was set up to test three different concentrations of the compounds,128,64 and 32 μ M, against biofilm formation. The formed biofilm was stained with crystal violet for twenty minutes and then washed thrice with distilled water. After this, crystal violet (CV) is added to dissolve into acetic acid and reading at 570 nm gives an idea about how much biomass has formed because higher OD means more biomass [35]. Each experiment was performed in triplicates; thus, % inhibition= [(OD control-OD sample)/OD control]x100 where OD stands for optical density.

2.4. Molecular docking

Molecular docking is defined as the process by which the interaction between small molecules and receptors can be studied at the molecular level. Many computational tools exist to help elucidate several kinds of physical interactions between organic molecules and receptor amino acids. In this work Auto Dock was used for performing molecular docking. The protein structure of S. aureus (PDB ID: 4DUH, Resolution: 1.50 Å) available on RCSB database has been downloaded and the protein was prepared prior to carrying out docking. Protein and ligand structures were prepared before carrying out molecular docking using Auto Dock. The protein was prepared by removing water molecules, adding polar hydrogen atoms and calculating Koll man charges using Chimera and Discovery Studio. Unwanted ligands were also removed for clean docking. Chem Draw was used to build structure of prepared compounds and its geometry optimized by MM2 energy minimization.

3. Results

N-propargylated intermediate (2) was synthesized by the alkylation of compound (1) with propargyl bromide in the presence of potassium carbonate under reflux in dry acetone. The reaction afforded a high yield (83%) of compound (2)) thus indicating efficient deprotonation and nucleophilic substitution at the nitrogen center, as shown schematically in Figure 1. IR: The terminal alkyne functionality is evidenced by its characteristic $\equiv C-H$ stretching 3311 (cm^{-1}) and $C \equiv C$ band 2128 (cm^{-1}); aromatic C–H, C=C stretching vibrations appear at their expected regions thereby supporting integrity for an indole framework within this molecule. (cm^{-1}) NMR: Displayed methylene protons adjacent to indole nitrogen δ 5.46, propargyl CH_2 group δ 4.17 which are consistent with successful N-alkylation having taken place. Signals for the alkyne carbons appeared at δ 81.36 and 74.14 along with well-resolved aromatic carbon peaks in the ^{13}C NMR spectrum, further supporting formation of compound (2). The prepared alkyne intermediate (2) was subjected to copper(I)-catalyzed azide-alkyne cycloaddition (CuAAC) with various organic azides to furnish the corresponding 1,4-disubstituted 1,2,3-triazole derivatives (3ta-3te). The $cuso_4$/sodium ascorbate system efficiently generates the active Cu(I) species in situ which allows for a highly selective reaction towards the 1,4-regioisomer [35]. All reactions were completed smoothly in ethanol-water(70-75°C) giving good yields (73-81%) thus demonstrating robustness of click reaction even with structurally diverse azides. Spectroscopically proven by appearance sharp singlet signal due triazole proton at δ 8.19-8 .38 on ^1H NMR spectra all derivatives formation triazole ring has been established. IR spectra showed a characteristic absorption of C-H stretching in triazole around 3110-3140 (cm^{-1}) along with the expected functional group absorptions depending on the substituent (O-H, N-H, sulfonamide, acetamide). Each derivative displayed additional diagnostic spectral features due to its substituent. Compound 3ta displayed a methoxy signal at δ 3.85 and a triazole linked CH_2 at δ 4.61 confirming formation of an ether linkage. In 3tb, amide NH at δ 9.97 and carbonyl stretch observed at 1687 (cm^{-1}) gives strong evidence about integrity for acetamide moiety. The phenolic derivative, 3tc exhibited downfield singlet (at δ 9.54) attributable to the phenolic OH.

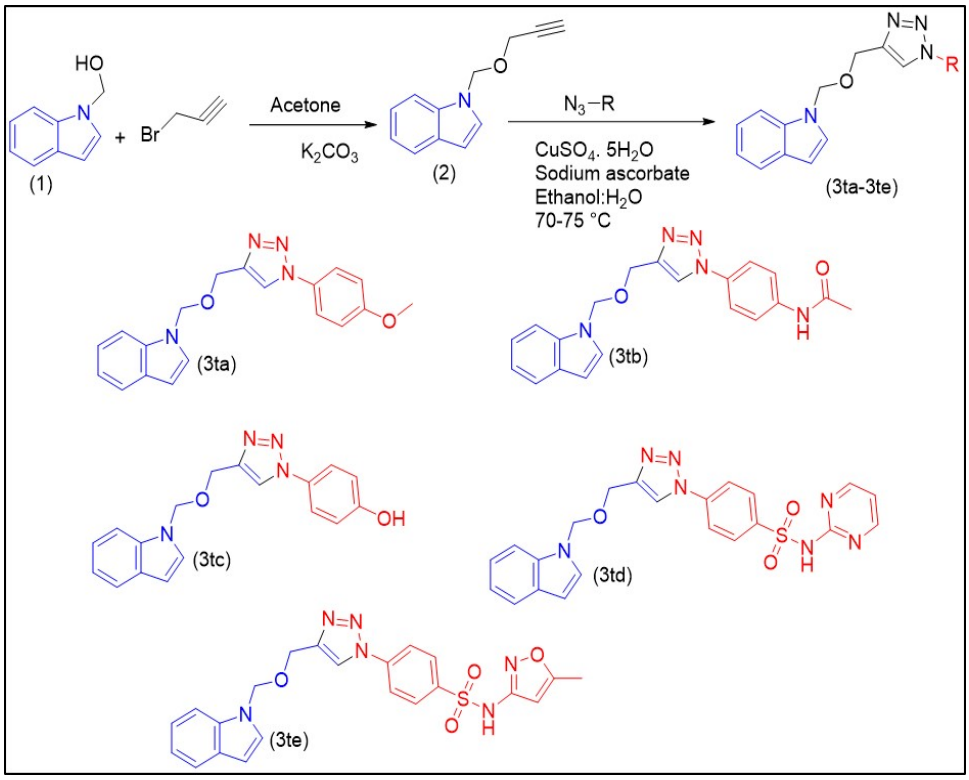

Figure 1: Preparation of new 1,2,3- triazole compounds (3ta-3te)

The sulfonamide compounds 3td and 3te showed intense N–H stretching bands in the IR around 3287 (cm^{-1}), and characteristic aromatic–sulfonamide carbon signals in the ^{13}C NMR. Compound 3te specifically displayed signals at δ 167.89 and 96.64 for the isoxazole carbons as well as a methyl resonating at δ 2.35, clearly indicating successful coupling of the heterocycle. All other spectral data obtained for synthesized triazole derivatives (3ta–3te) were completely consistent with their proposed structures demonstrating that an efficient N-propargylation followed by a highly regioselective CuAAC click cycloaddition can serve as a reliable synthetic route to generate structurally diverse indole–triazole hybrids. The good yields clean conversions and strong spectroscopic agreement make this methodology very attractive toward constructing biologically oriented heterocycles for further pharmacological evaluation.

3.1. Antibacterial Evaluation

A clear structure activity relationship was observed among the synthesized triazole–indole hybrids (3ta–3te) with obvious differences in potency among the tested bacterial strains, as shown in Figure 2 Among this series, compound 3te exhibited the highest activity with low MIC values against S. aureus (6.21 μ M), B. subtilis (8.13 μ M), and E. coli (25.45 μ M). The corresponding MBC values for this compound ranged from 24.25 to 100 μ M and indicated a strong bactericidal effect thus suggesting that antibacterial activity is greatly enhanced by methyl-isoxazole–sulfonamide moiety present in 3te. Compound 3td also exhibited high activity particularly on Gram positive strains with MIC values of 12.32 μ M and 15.12 μ M against S. aureus and B. subtilis respectively thus showing contribution made by

pyrimidine-sulfonamide substituent towards enhanced potency. On the other hand derivatives 3ta bearing methoxy, acetamide or phenolic substituents showed only moderate to weak activities with MIC values ranging from 25,.41-100,.35 μ M on Gram positive bacteria and very much lower activities against E.coli 120-278 μ m). The uniformly high values of MBC for these compounds (160–¿400 μ M) clearly support mainly bacteriostatic action. The lower susceptibility in E.coli across the series is consistent with the intrinsic resistance associated with permeability barriers of outer membranes in Gram-negative bacteria. In general, results have shown that antibacterial activity of sulfonamide containing triazole analogs 3td and 3te are much higher relative to other analogs within the series. Ciprofloxacin still remains one among most active reference drugs tested so far but both compounds, especially 3te exhibited promising low MIC/MBC values hence structural incorporation heteroaromatic sulfonamide fragments into triazole–indole scaffold significantly enhances antibacterial potency might be further optimized.

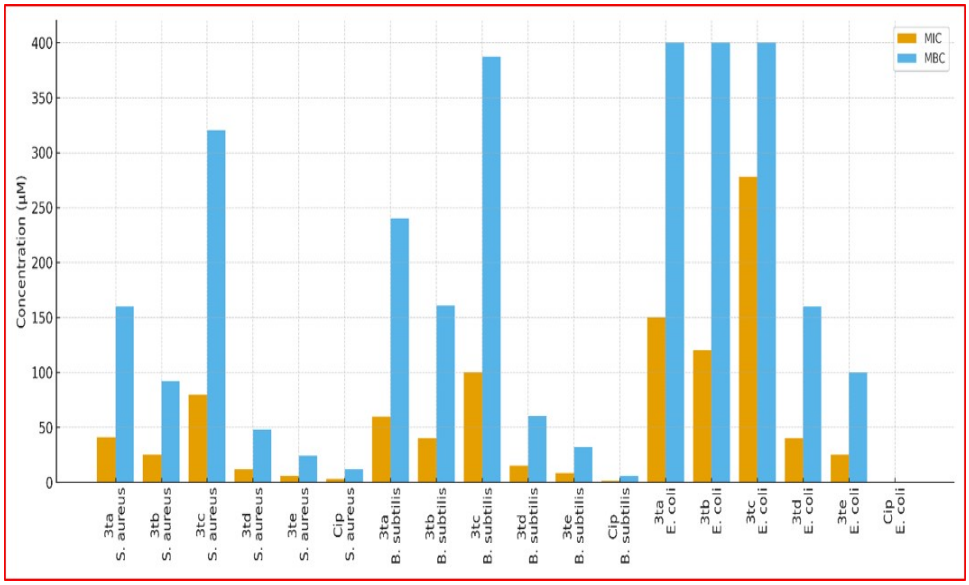

Figure 2: Comparative representation of MIC and MBC values of the synthesized compounds (3ta–3te) against *S. aureus, B. subtilis*, and *E. coli*, presented alongside ciprofloxacin as the reference drug

3.2. Molecular Docking Studies

The molecular docking analysis of synthesized triazole derivatives (3ta–3te) against S. aureus target protein (PDB: 4DUH) exhibited differences in binding affinity, types of interactions and RMSD values which collectively explain their potential antibacterial activity. All the compounds assumed stable docked poses with RMSD values less than 2 Å thereby indicating good docking conformations. Among all; compound 3te showed highest binding affinity having a docking score value as-8.3986 kcal·mol^{-1} followed by compounds 3td (-8.0728 kcal·mol^{-1}) and 3tb (-7.9716 kcal·mol^{-1}). This is also in correlation with its experimentally determined antibacterial activities where these two compounds have shown lowest MIC and MBC values next to them respectively Table 1. The interaction profile supports this trend further. A key hydrogen bond donor interaction was observed between compound 3te and ASP73, Δ E = -0.9 kcal·mol^{-1} at a distance of 3.27 Å together with a stabilizing π-cation interaction with ARG136. Both residues are within the active pocket of 4DUH and have been reported as ligand-anchoring residues. Similarly, a number of strong hydrogen bond acceptor interactions were observed between 3td and ARG136, Δ E = -2.5 and -0.8 kcal·mol^{-1}) in addition to a π-H interaction with THR165 Table 1.

Table 1: Molecular docking scores and binding interactions of ligands (3ta-3te) against (PDB: 4DUH)

Ligand	RMSD (Å)	Dock Score E(kcal·mol^{-1})	Interaction type	Δ E(kcal·mol^{-1}) per interaction	Distance (Å)	Residue / Partner
3ta	1.6571	-7.7981	pi-H	-0.6	3.77	LYS 103
3tb	1.5666	-7.9716	H-B-D	-0.9	2.85	ASP 73
3tc	1.5131	-7.0726	H-B-D	-3.6	2.90	ASP 73
			pi-H	-0.8	4.03	ASN 46
3td	1.4018	-8.0728	H-B-A	-0.8	3.37	ARG 136
			H-B-A	-2.5	3.15	ARG 136
			pi-H	-0.6	4.03	THR 165
3te	1.07829	-8.3986	H-B-D	-0.9	3.27	ASP 73
			pi-cation	-0.6	3.39	ARG 136

The presence of several possible interactions and their favorable energies most probably explain its high docking score as well as biological potency. Compounds 3tb and 3tc also formed hydrogen bonds with ASP73, though the interaction energies were considerably lower, reflected in their moderate docking scores. For 3tc there is a minor stabilizing(π-H) interaction with ASN46. (δ E=-0.8kcal·mol^{-1}) The compound showing lowest binding energy (-7.7981 kcal·mol^{-1}), that is 3ta engaged only a single (π-H) interaction with LYS103 thus indicating poor anchoring within active site consistent with weaker antibacterial performance. These results can be visually confirmed from

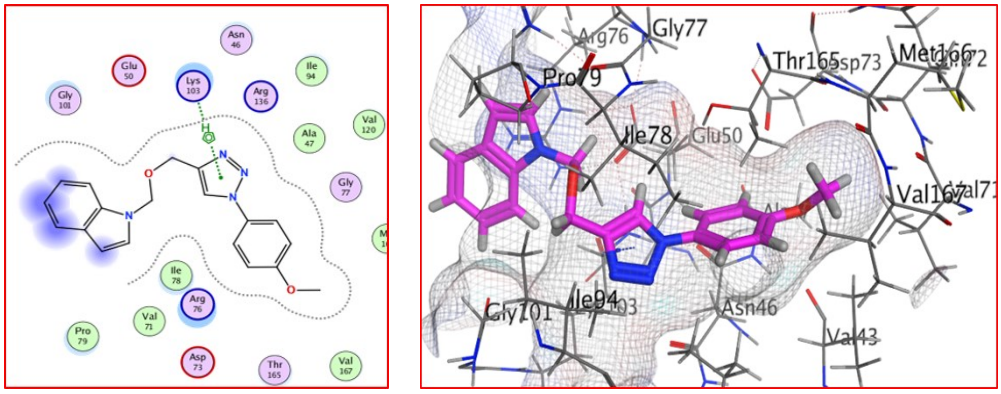

Figure 3: 2D and 3D interaction (3ta) with active site of 4DUH

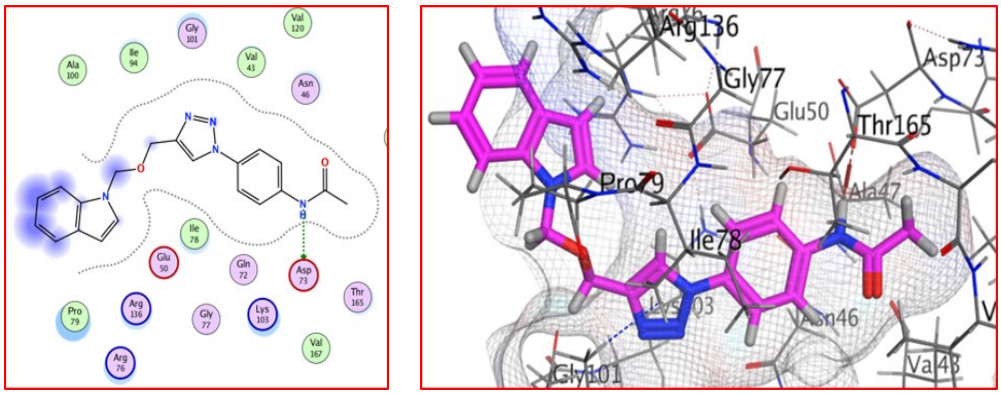

Figure 4: 2D and 3D interaction (3tb) with active site of 4DUH

2D&3D interaction plots Figures 3, 4, 5, 5, 6, 7 Where it's clearly seen that most active compounds particularly, 3te form stronger and a greater number of interactions involving catalytic residues of 4DUH. Summing up all these results, the heterocycles are electron-rich and contain functional groups capable of hydrogen bonding and π-cation interactions with high binding affinity reflected in better antibacterial activity. A clear SAR trend is provided by the outcome of docking that shows 3te as a very potential candidate because it optimally orients within the active site where strong stabilizing interactions with important amino acid residues take place.

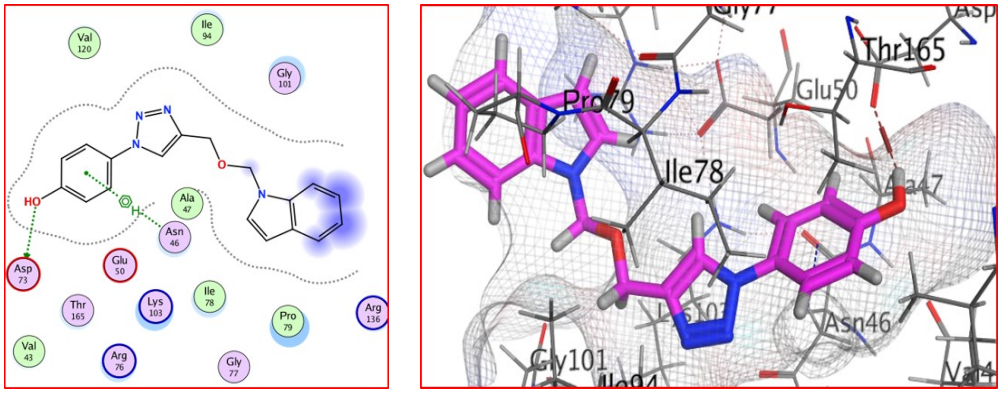

Figure 5: 2D and 3D interaction (3tc) with active site of 4DUH

3.3. Pharmacokinetic, Physicochemical 1,2,3-triazole compounds (3ta–3te)

The presence of several possible interactions and their favorable energies most probably explain its high docking score as well as biological potency. Compounds 3tb and 3tc also formed hydrogen bonds with ASP73, though the interaction energies were considerably lower, reflected in their moderate docking scores. For 3tc there is a minor stabilizing (π-H) interaction with ASN46 (δE=-0.8kcal·mol^{-1}). The compound showing lowest binding energy (-7.7981 kcal·mol^{-1}), that is 3ta engaged only a single (π-H) interaction with LYS103 thus indicating poor anchoring within active site consistent with weaker antibacterial performance. These results can be visually confirmed from 2D & 3D interaction plots Figures 3, 4, 5, 5, 6, 7 where it's clearly seen that most active compounds particularly, 3te & d form stronger and a greater number of interactions involving catalytic residues of 4DUH. Summing up all these results, the heterocycles are electron-rich and contain functional groups capable of hydrogen bonding and π-cation interactions with high binding affinity reflected in better antibacterial activity. A clear SAR trend is provided by the outcome of docking that shows 3te as a very potential candidate because it optimally orients within the

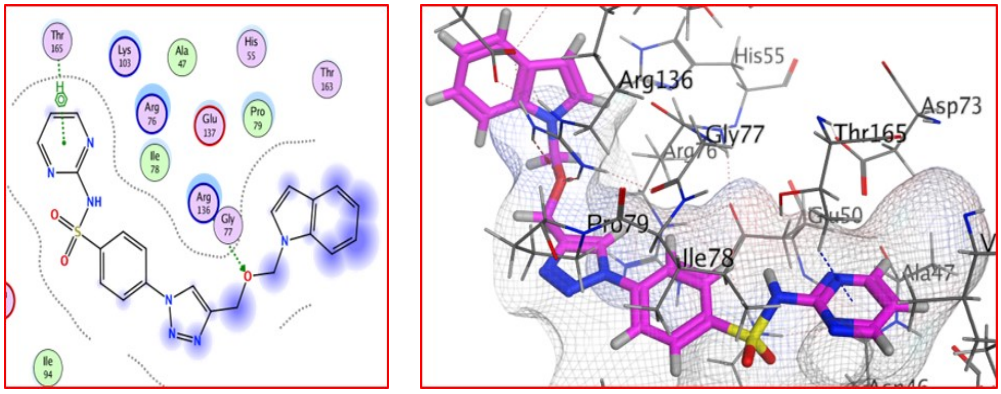

Figure 6: 2D and 3D interaction (3td) with active site of 4DUH

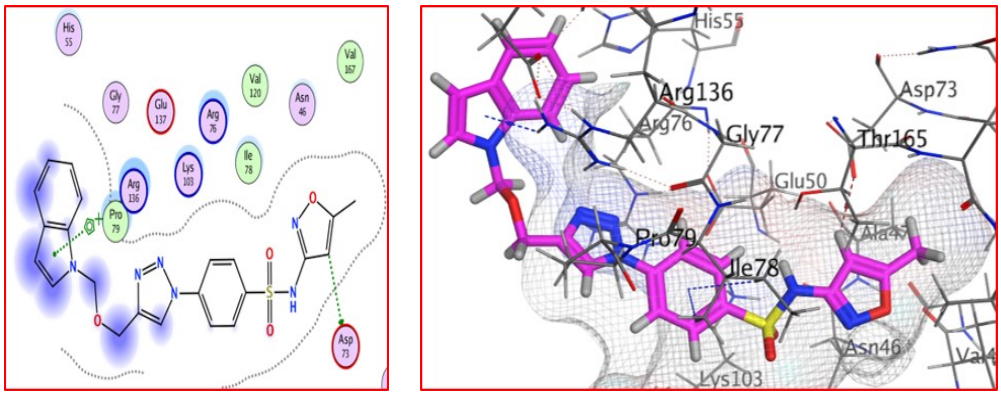

Figure 7: 2D and 3D interaction (3te) with active site of 4DUH

active site where strong stabilizing interactions with important amino acid residues take place.

Table 2: Predicted Physicochemical, Pharmacokinetic, and Drug-Likeness Properties of Compounds 3ta–3te

Molecule	3te	3td	3tc	3tb	3ta
MW	464.5	461.5	320.35	361.4	334.37
H-bond acceptors	7	7	4	4	4
H-bond donors	1	1	1	1	0
TPSA	125.45	125.2	65.1	73.97	54.1
iLOGP	2.63	1.81	2.63	2.92	3.21
ESOL Log S	-4.35	-4	-3.68	-3.44	-3.88
ESOL Class	Moderately soluble	Moderately soluble	Soluble	Soluble	Soluble
Ali Log S	-4.82	-4.24	-3.49	-3.2	-3.6
GI absorption	High	High	High	High	High
BBB permeant	No	No	Yes	Yes	Yes
CYP1A2 inhibitor	No	No	Yes	Yes	Yes
CYP2C19 inhibitor	Yes	Yes	Yes	Yes	Yes
CYP2C9 inhibitor	Yes	Yes	Yes	Yes	Yes
CYP2D6 inhibitor	No	No	Yes	Yes	Yes
CYP3A4 inhibitor	Yes	Yes	Yes	Yes	Yes
log Kp (cm/s)	-7.33	-7.71	-6.49	-7.07	-6.34
Lipinski # violations	0	0	0	0	0
Veber # violations	0	0	0	0	0
Bioavailability Score	0.55	0.55	0.55	0.55	0.55

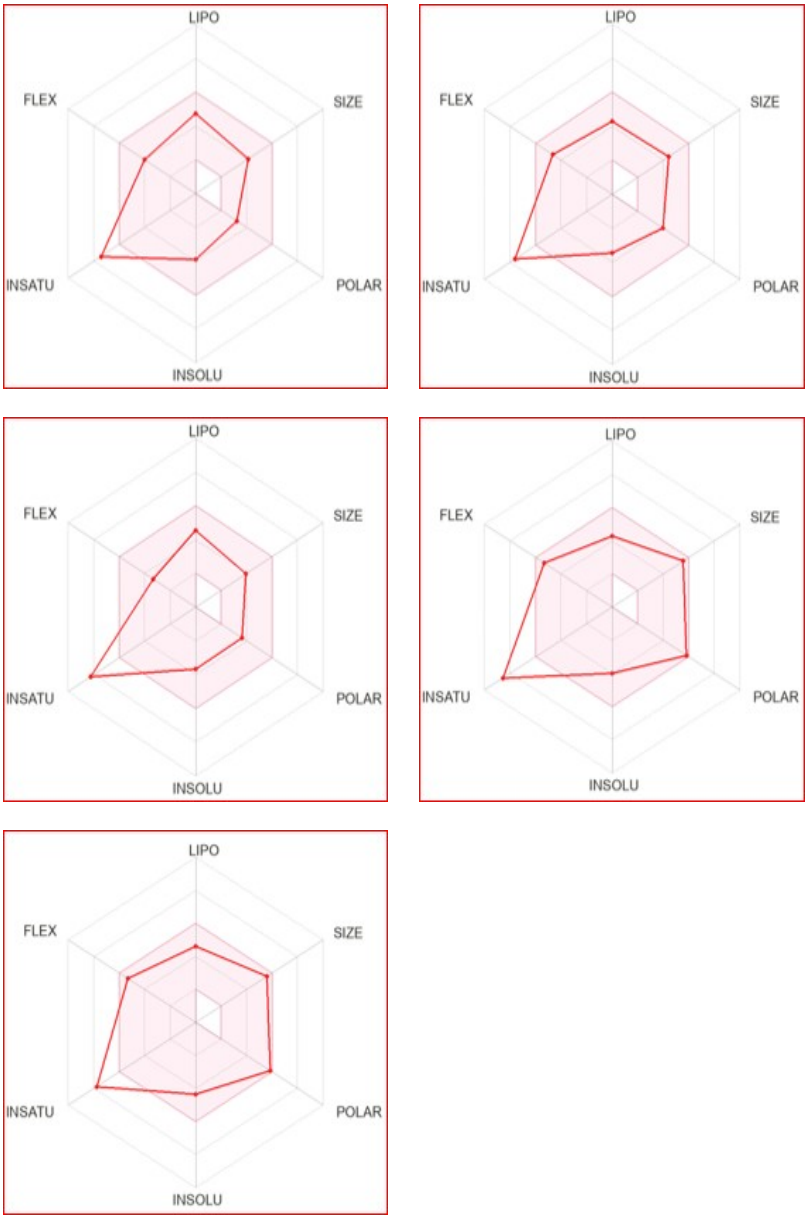

Figure 8: Radar chart of synthesis compounds (3ta-3te)

4. Conclusion

In this work, a new series of indole–1,2,3-triazole hybrid molecules (3ta–3te) was successfully designed, synthesized, and characterized using a reliable two-step strategy involving N-propargylation followed by Cu(I)-catalyzed click cycloaddition. All synthesized compounds were obtained in good yields and fully confirmed by spectroscopic analyses. Biological evaluation demonstrated that structural modification significantly influenced antimicrobial potency, with sulfonamide-bearing derivatives especially compound 3te exhibiting the most potent antibacterial and antibiofilm activities, supported by low MIC/MBC values. Molecular docking studies further validated these findings, showing that 3te and 3td possess the highest binding affinities toward the S. aureus target protein (4DUH), forming key stabilizing interactions with essential catalytic residues. ADMET and drug-likeness assessments revealed favorable pharmacokinetic profiles and compliance with major drug ability rules, suggesting their suitability for further optimization. Overall, this study highlights the indole–triazole scaffold as a promising chemotype for developing new antimicrobial agents, with compound 3te emerging as a strong lead candidate for future in vivo and mechanistic studies aimed at combating antimicrobial resistance.

Article Information

Disclaimer (Artificial Intelligence): The author(s) hereby declare that NO generative AI technologies such as Large Language Models (ChatGPT, COPILOT, etc.), and text-to-image generators have been used during writing or editing of manuscripts.

Competing Interests: Authors have declared that no competing interests exist.

References

[1] S. K. Ahmed, S. Hussein, K. Qurbani, R. H. Ibrahim, A. Fareeq, K. A. Mahmood, and M. G. Mohamed. Antimicrobial resistance: impacts, challenges, and future prospects. *J. Med. Public Health*, 2:100081, 2024. doi:10.1016/j. glmedi.2024.100081.

[2] A. Y. Hwang and J. G. Gums. The emergence and evolution of antimicrobial resistance: impact on a global scale. *Bioorg. Med. Chem.*, 24(24):6440–6445, 2016. doi:10.1016/j.bmc.2016.04.027.

[3] R. M. Donlan and J. M. Costerton. Biofilms: survival mechanisms of clinically relevant microorganisms. *Clin. Microbiol. Rev.*, 15(2): 167–193, 2002. doi:10.1128/cmr.15.2.167-193.2002.

[4] F. Sun, F. Qu, Y. Ling, P. Mao, P. Xia, H. Chen, and D. Zhou. Biofilm-associated infections: antibiotic resistance and novel therapeutic strategies. *Future Microbiol*, 8(7):877–886, 2013. doi:10.2217/fmb.13.58.

[5] S. Miquel, R. Lagrafeuille, B. Souweine, and C. Forestier. Anti-biofilm activity as a health issue. *Front. Microbiol.*, 7:592, 2016. doi:10.3389. fmicb.2016.00592.

[6] A. Vashistha, N. Sharma, Y. Nanaji, D. Kumar, G. Singh, R. P. Barnwal, and A. K. Yadav. Quorum sensing inhibitors as therapeutics: bacterial biofilm inhibition. *Bioorg. Chem.*, 136:106551, 2023. doi:10.1016/j.bioorg.2023.106551.

[7] World Health Organisation. Antimicrobial Resistance WHO. 2024. URL https://www.who.int/news-room/fact-sheets/detail/antimicrobial-resistance.

[8] N. Poonia, K. Lal, and A. Kumar. Design, synthesis, antimicrobial evaluation and in silico studies of symmetrical bis (urea-1,2,3-triazole) hybrids. *Res. Chem. Intermed*, 47:1087–1103, 2021. doi:10.1007/s11164-020-04318-1.

[9] S. Mudenda, B. Chabalenge, V. Daka, R. L. Mfune, K. I. Salachi, S. Mohamed, W. Mufwambi, M. Kasanga, and S. K. Matafwali. Global strategies to combat antimicrobial resistance: a one health perspective. *Pharmacol. Pharm.*, 14(8):271–328, 2023. doi:10.4236/pp.2023.148020.

[10] R. R. Uchil, G. S. Kohli, V. M. KateKhaye, and O. C. Swami. Strategies to combat antimicrobial resistance. *J. Clin. Diagn. Res: JCDR*, 8(7):ME01, 2014. https://doi.org/10.7860/JCDR/2014/8925.4529.

[11] K. W. K. Tang, B. C. Millar, and J. E. Moore. Antimicrobial resistance (AMR). *Br. J. Biomed. Sci.*, 80:11387, 2023. doi:10.3389/bjbs.2023.11387.

[12] A. Kumar, K. Lal, M. Yadav, S. Kumar, M. B. Singh, and K. Kumari. Isatin-semicarbazone linked acetamide 1, 2, 3-triazole hybrids: synthesis, antimicrobial evaluation and docking simulations. *J. Mol. Struct.*, 1287:135660, 2023. doi:10.1016/j.molstruc.2023.135660.

[13] N. George, M. J. Akhtar, K. A. Al Balushi, and S. A. Khan. Rational drug design strategies for the development of promising multi-target directed indole hybrids as anti- alzheimer agents. *Bioorg. Chem.*, 127:105941, 2022. doi:10.1016/j.bioorg.2022.105941.

[14] A. Kumari and R. K. Singh. Medicinal chemistry of indole derivatives: current to future therapeutic prospectives. *Bioorg. Chem.*, 89: 103021, 2019. doi:10.1016/j.bioorg.2019.103021.

[15] B. Priya, D. Utreja, S. Sharma, and G. Kaur. Synthesis and antimicrobial activities of indole-based schiff bases and their metal complexes: a review. *Curr. Org. Chem.*, 27(11):941–961, 2023. doi:10.2174/1385272827666230901140611.

[16] M. Yang, J. Li, and P. R. Chen. Transition metal-mediated bioorthogonal protein chemistry in living cells. *Chem. Soc. Rev.*, 43: 6511–6526, 2014. doi:10.1039/C4CS00117F.

[17] J. Kaur, M. Saxena, and N. Rishi. An overview of recent advances in biomedical applications of click chemistry. *Bioconjugate Chem.*, 32(8):1455–1471, 2021. doi:10.1021/acs.bioconjchem.1c00247.

[18] A. Kumar, V. Kumar, P. Singh, R. K. Tittal, and K. Lal. Ionic liquids for green synthesis of 1,2,3-triazoles: a systematic review. *Green Chem.*, 26 , https:3565–3594, 2024. doi:10.1039/D3GC04898E.

[19] J. Hou, X. Liu, J. Shen, G. Zhao, and P. G. Wang. The impact of click chemistry in medicinal chemistry. *Expert Opin. Drug Discov.*, 7 (6):489–501. doi:10. 1517/17460441.2012.682725.

[20] R. Huisgen, R. Grashey, and J. Sauer. Cycloaddition reactions of alkenes. *The Alkenes*, 1:739–953, 1964. doi:10.1002/9780470771044.ch11.

[21] H. C. Kolb, M. G. Finn, and K. B. Sharpless. Click chemistry: diverse chemical function from a few good reactions. *Angew. Chem. Int. Ed. Engl.*, 40(11):2004–2021, 2001. doi:10.1002/1521-3773(20010601.

[22] N. M. Aljamali, R. M. U. Mahmood, and R. A. Baqi. Review on preparation and application fields of triazole tetrazole derivatives. *Int. J. Anal. Chem.*, 6(1):50–60, 2020.

[23] A. Kumar, K. Lal, V. Kumar, M. Murtaza, S. Jaglan, A. K. Paul, S. Yadav, and K. Kumari. Synthesis, antimicrobial, antibiofilm and computational studies of isatin- semicarbazone tethered 1,2,3-triazoles. *Bioorg. Chem.*, 133:106388, 2023. doi:10.1016/j.bioorg.2023.106388.

[24] A. Kumar, K. Lal, L. Kumar, A. Kumar, and R. K. Naveen. Tittal, phenylhydrazone linked 1,2,3-triazole hybrids: synthesis, antimicrobial evaluation and docking studies as dual inhibitors of DNA gyrase and lanosterol 14 demethylase. *Res. Chem. Intermed*, 48(12):5089–5111, 2022. doi:10.1007/s11164-022-. 04849-9.

[25] L. Kumar, K. Lal, A. Kumar, and A. Kumar. Synthesis, antimicrobial evaluation and docking studies of oxazolone-1, 2, 3-triazole-amide hybrids. *Res. Chem. Intermed*, 47:5079–5097, 2021. doi:10.1007/s11164-021-04588-3.

[26] M. Yadav, K. Lal, A. Kumar, P. Singh, V. K. Vishvakarma, and R. Chandra. Click reaction inspired synthesis, antimicrobial evaluation and in silico docking of some pyrrole- chalcone linked 1,2,3-triazole hybrids. *J. Mol. Struct.*, 1273:134321, 2023. doi:10.1016/j.molstruc.2022.134321.

[27] K. Lal and P. Yadav. Recent advancements in 1,4-disubstituted 1H-1,2,3-triazoles as potential anticancer agents, Anti-Cancer Agents Med. *Chem. (Formerly Current Medicinal Chemistry-Anti-Cancer Agents)*, 18(1):21–37, 2018. doi:10.2174/1871520616666160811113531.

[28] P. Yadav, K. Lal, A. Kumar, S. K. Guru, S. Jaglan, and S. Bhushan. Green synthesis and anticancer potential of chalcone linked-1,2,3-triazoles. *Eur. J. Med. Chem.*, 126:944–953, 2017. doi:10.1016/j.ejmech.2016.11.030.

[29] Y. W. He, C. Z. Dong, J. Y. Zhao, L. L. Ma, Y. H. Li, and H. A. Aisa. 1,2,3-Triazole- containing derivatives of rupestonic acid: click-chemical synthesis and antiviral activities against influenza viruses. *Eur. J. Med. Chem.*, 76:245–255, 2014. doi:10.1016/j.ejmech.2014.02.029.

[30] N. Batra, V. Rajendran, D. Agarwal, I. Wadi, P. C. Ghosh, R. D. Gupta, and M. Nath. Synthesis and antimalarial evaluation of 1,2,3-triazole-tethered sulfonamide- berberine hybrids. *ChemistrySelect*, 3(34):9790–9793, 2018. doi:10.1002/slct.201801905.

[31] S. Jana, S. Iram, J. Thomas, M. Q. Hayat, C. Pannecouque, and W. Dehaen. Application of the triazolization reaction to afford dihydroartemisinin derivatives with anti- HIV activity molecules 22(2) (2017) 303. s22020303. doi:10.3390/molecule.

[32] Z. Fallah, M. Tajbakhsh, M. Alikhani, B. Larijani, M. A. Faramarzi, M. M. Khanaposhtani, H. Hamedifar, and M. Mahdavi. A review on synthesis, mechanism of action, and structure-activity relationships of 1,2,3-triazole-based -glucosidase inhibitors as promising anti-diabetic agents. *J. Mol. Struct.*, 1255:132469, 2022. doi:10.1016/j.molstruc.2022.132469.

[33] A. P. S. Raman, M. Aslam, A. Awasthi, A. Ansari, P. Jain, K. Lal, K. Kumari, I. Bahadur, and P. Singh. An updated review on 1,2,3-/1,2,4-triazoles: synthesis and diverse range of biological potential. *Mol. Diver*, 29:899–964, 2024. https://doi. org/10.1007/s11030-024-10858-0.

[34] M. Chauhan, A. Saxena, and B. Saha. An insight in anti-malarial potential of indole scaffold: a review. *Eur. J. Med. Chem.*, 218: 113400, 2021. doi:10.1016/j.ejmech.2021.113400.

[35] M. Verma, M. Tripathi, A. K. Saxena, and K. Shanker. Antiinflammatory activity of novel indole derivatives. *Euro. J. Med. Chem.*, 29 (12):941–946, 1994. https://doi.org/10.1016/0223-5234(94)90193-7.